

# PHOTOMASK

BACUS—The international technical group of SPIE dedicated to the advancement of photomask technology.

EMLC17 Best Paper

## Depth-profiling of vertical material contrast after VUV exposure for contact-free polishing of 3D polymer micro-optics

**R. Kirchner**, Technische Universität Dresden, Institute of Semiconductors and Microsystems, 01062 Dresden, Germany

**R. Hoekstra, N. Chidambaram, and H. Schiff**, Paul Scherrer Institute, Laboratory for Micro- and Nanotechnology, 5232 Villigen PSI, Switzerland

### ABSTRACT

We characterize the impact of high-energy, 172 nm vacuum ultraviolet photons on the molecular weight and the glass transition temperature of poly(methyl methacrylate). We found that the molecular weight is reduced strongly on the surface of the exposed samples with a continuous transition towards the unexposed bulk material being located below the modified region. The glass transition temperature was found to be significantly lowered in the exposed region to well below 50°C compared to that of the 122°C of the bulk region. We could use this material contrast to selectively reflow the top surface of the exposed samples only. This allowed us to create ultra-smooth micro-optical structures by postprocessing without influencing the overall geometry that is required for the optical functionality.

### 1. Introduction

Creating material contrast is the basic principle of lithography since the fabrication of integrated electronic circuits. To transfer the image of a mask into a resist material, an exposure or writing process creates a latent image in terms of different solubility of the resist regions due to modification of the resist by high-energy radiation. This radiation comprises in most cases photons, electrons or ions. To create a topography contrast, this latent image is transformed into a physical topography during the development process by chemicals that selectively remove parts of the latent image in the resist. For example, for a positive tone resist the solubility in the developer is enhanced and the exposed regions are dissolved and removed. This enhanced solubility can be among others due to a reduced molecular weight of a linear polymer in a solvent. A well-known example is poly(methyl methacrylate) (PMMA) often used as positive tone electron beam lithography (EBL) resist. Upon exposure with high-energy electrons, the molecular weight  $M_w$  is significantly

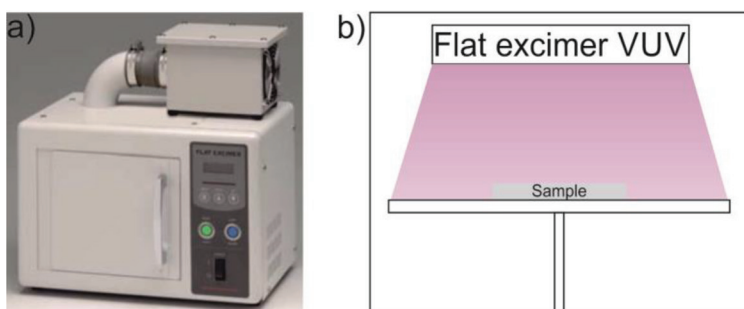


Figure 1. a) Photograph and b) schematic of the exposure setup with a 172 nm wavelength, flat excimer lamp.

BACUS

N • E • W • S

OCTOBER 2017  
VOLUME 33, ISSUE 10

TAKE A LOOK  
INSIDE:

INDUSTRY BRIEFS  
— see page 8

CALENDAR  
For a list of meetings  
— see page 9

SPIE.

10446-18

# EDITORIAL

## “In this corner of the mask world”

**Naoya Hayashi, Dai Nippon Printing Co., Ltd.**

Last November, 2016, an animated movie titled “In the corner of the world” started showing in Japan. At first, only 63 theatres showed it, but finally it expanded to 360 and recorded the revenue of more than 20 million dollars, quite high for such small scale movie, and got the Best Animated Movie of 2016 Japan Academy Award. It started showing in the US this summer, and got good feedback so far. This movie described the life of the common people under very difficult circumstances, during the last world war. They tried to continue the ordinary days, eat, wash and clean, loving each other, by using limited tools and materials around them. Their strong will, even if sometimes destroyed by war, won the sympathy of the audiences.

In our photomask industry, there are also people who have showed the constant but strong effort for many years under the challenging circumstances, and great contribution for the industry. This year, BACUS Committee awarded such persons as BACUS Lifetime Achievement Award and BACUS Prize.



Dr. Hiroaki Morimoto received the BACUS Lifetime Achievement Award. Morimoto-san spent more than 25 years in lithography and mask technology at Mitsubishi Electronics. Highlights of his work include the ion beam repair system that was commercialized by Seiko Instrument and the invention of the attenuated phase-shifting mask with a single-layer absorptive shifter which is still used in production. He was once the manager of SELETE, a project for mask technology development for VUV and EUV in Japan. Morimoto-san joined Toppan Printing in 2003, and currently the Meister, Senior Chief Researcher. Morimoto-san is also a famous movie director of Photomask Japan entertainment together with me!



Dr. Hans Loeschner and Dr. Elmar Platzgummer received the BACUS Prize in recognition of their contribution to the photomask industry through their work and influence to develop and commercialize Multi-Beam photomask lithography tool.

Dr. Hans Loeschner received a Ph.D. in Physics from the University of Vienna. After completing his PhD in 1976, he worked till 1983 at a former Viennese company on ion beam resistless chip fabrication. Hans co-founded IMS Nanofabrication AG in 2006, focusing on multi-beam lithography and nanopatterning, and serves as its Chief Scientific Officer. He is also a Co-Founder of the Erwin Schroedinger Society for Nanosciences. In 2012 he received the “MNE Fellowship Award” for the advancements of electron and ion beam technologies.

Dr. Elmar Platzgummer received his Physics Diploma 1995 and his PhD 1999 from Vienna University of Technology. He joined IMS in 1999 and has taken a key role in the development of IMS's multi-beam technology and its application fields. In Oct 2005 he became CTO and COO of IMS, and in this role built IMS's team of experts and realized several RandD tools and prototype systems for the industry and in the framework of EU funded projects. Since Oct 2012, Elmar is Chief Executive Officer of IMS Nanofabrication AG.

With their excellent efforts, IMS Nanofabrication released the world first Multi-Beam Mask Writer, MBMW-101, in 2016 for high volume production of 7nm node and beyond.

Congratulations! Their achievements have been and will be contributing to the photomask industry for long time.

Why all of them hold a carrot pen in their photos? They were very important casts of my last movie titled “eUvTOPIA”, based on Disney’s “ZOOTOPIA”.

Next movies from “Morimoto Film” and me? Coming soon! Next April at PMJ 2018! Photomask Forever!!



**N • E • W • S**

BACUS News is published monthly by SPIE for BACUS, the international technical group of SPIE dedicated to the advancement of photomask technology.

**Managing Editor/Graphics** Linda DeLano

**Advertising** Melissa Farlow

**BACUS Technical Group Manager** Marilyn Gorsuch

### ■ 2017 BACUS Steering Committee ■

**President**

**Jim N. Wiley, ASML US, Inc.**

**Vice-President**

**Frank E. Abboud, Intel Corp.**

**Secretary**

**Shane Palmer, Nikon Research Corp. of America**

**Newsletter Editor**

**Artur Balasinski, Cypress Semiconductor Corp.**

**2017 Annual Photomask Conference Chairs**

**Peter D. Buck, Mentor Graphics Corp.**

**Emily Gallagher, IMEC**

**International Chair**

**Uwe F. W. Behringer, UBC Microelectronics**

**Education Chair**

**Frank E. Abboud, Intel Corp.**

**Members at Large**

**Michael D. Archuletta, RAVE LLC**

**Brian Cha, Samsung Electronics Co., Ltd.**

**Jerry Cullins, HOYA Corp.**

**Derren Dunn, IBM Corp.**

**Thomas B. Faure, GLOBALFOUNDRIES Inc.**

**Aki Fujimura, DS2, Inc.**

**Brian J. Grenon, Grenon Consulting**

**Jon Haines, Micron Technology Inc.**

**Naoya Hayashi, Dai Nippon Printing Co., Ltd.**

**Bryan S. Kasproicz, Photonics, Inc.**

**Patrick M. Martin, Applied Materials, Inc.**

**Jan Hendrik Peters, bmbg consult**

**Moshe Preil, KLA-Tencor Corp.**

**Douglas J. Resnick, Canon Nanotechnologies, Inc.**

**Thomas Scheruebl, Carl Zeiss SMT GmbH**

**Thomas Struck, Infineon Technologies AG**

**Bala Thumma, Synopsys, Inc.**

**Anthony Vacca, Automated Visual Inspection**

**Michael Watt, Shin-Etsu MicroSi Inc.**

**Larry S. Zurbrick, Keysight Technologies, Inc.**

**SPIE.**

P.O. Box 10, Bellingham, WA 98227-0010 USA

Tel: +1 360 676 3290

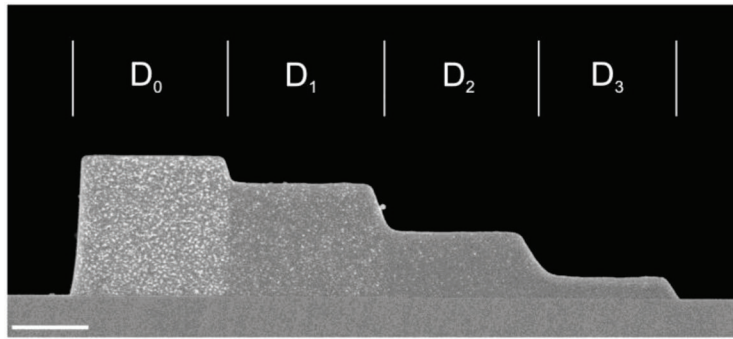
Fax: +1 360 647 1445

www.SPIE.org

help@spie.org

©2017

All rights reserved.



Dose $D_x$ ( $\mu\text{C}/\text{cm}^2$ )	$M_{wx}$ (kg/mol)	$T_{gx}$ ( $^{\circ}\text{C}$ )
0	91.2	122
120	29.2	106
200	18.0	101
270	13.0	97

Figure 2. Profile of an electron beam exposed sample with increasing dose from the first step  $D_0$  until the last step  $D_3$  ( $D_0 = 0 \mu\text{C}/\text{cm}^2$ ,  $D_1 = 120 \mu\text{C}/\text{cm}^2$ ,  $D_2 = 200 \mu\text{C}/\text{cm}^2$ ,  $D_3 = 270 \mu\text{C}/\text{cm}^2$ ). Outside the steps, a larger dose (dose-to-clear) was applied. The granularity of the cleaved facets is governed by the  $M_w$  of the respective region. The tabulated data is based on Ref.<sup>[3]</sup>. (Scale bar 1  $\mu\text{m}$ )

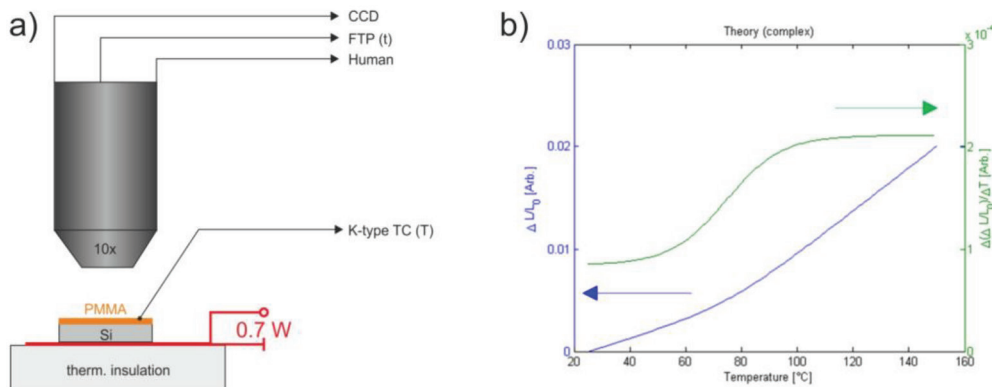


Figure 3. a) Measurement setup and b) exemplary graph of the relative film thickness increase and the first derivative of this versus the temperature defined as CTE. The complex theoretical film used here for visualization has a central  $T_g$  of  $75^{\circ}\text{C}$  and a width of the transition region of  $40^{\circ}\text{C}$ .

reduced due to electron induced chain scission<sup>[1]</sup>. As shown in several publications, the reduced  $M_w$  in PMMA leads to a reduced glass transition temperature  $T_g$  especially when it falls below a certain critical molecular weight<sup>[2-4]</sup>. By defining a contrast in  $T_g$ , a much broader diversity of micro-lenses can be for example created compared to the classical reflow process<sup>[5,6]</sup>. A lateral contrast of  $T_g$  allows to create an asymmetric polymer reflow profile<sup>[3,7,8]</sup>. In contrast, a vertical  $T_g$  contrast as used in this work enables to selectively initiate polymer relocation on the surface of a thick polymer film or structure while the bulk of this polymer structure will remain unaffected<sup>[4]</sup>. This can be for example used to create ultra-smooth micro optics<sup>[4,9-11]</sup>.

The glass transition region is a special region because many physical properties are significantly different below and above this region while a gradual change of these properties take place within this region. One such a particular property is the thermal expansion that can be described by the linear coefficient of thermal expansion (CTE). The CTE as well as the refractive index are significantly different below and above the  $T_g$  region due to the free volume increase during glass transition. The thickness and, thus, also the CTE is well accessible using optical probes such as ellipsometry<sup>[12]</sup> or white light reflectometry as used in this work.

We characterize the exposure impact on the  $M_w$  based on scanning electron micrographs and on the  $T_g$  based on measurement of the thermal expansion. We further demonstrate the reduction of the surface roughness based on the confined modification of the  $T_g$  of the surface of a micro-optical diffuser and a micro-prism array.

## 2. Materials and Methods

### 2.1 172 nm VUV exposure

The surface of PMMA samples was exposed by 172 nm vacuum ultraviolet (VUV) photons using a commercial lab setup (EX-mini, Hamamatsu Photonics K.K.) under ambient conditions with a short distance of 3 mm and 10 mm to the lamp housing to ensure a high enough photon impact (Fig. 1). The nominal VUV output power is about  $50 \text{ mW}/\text{cm}^2$ . The photon energy for the used distance was about  $16.3 \text{ mW}/\text{cm}^2$  and  $5.5 \text{ mW}/\text{cm}^2$  based on a calibration curve for 3 mm and 10 mm, respectively. Typical exposure times were up to 60 s. The PMMA samples were prepared by spin-coating of PMMA120k (micro resist technology GmbH) and post-apply baked at  $140^{\circ}\text{C}$  for 2 min. Subsequently, the samples were exposed and immediately characterized by the methods mentioned below.

### 2.2 SEM cross sections

The mechanical properties of PMMA strongly depend on the  $M_w$ . A low  $M_w$  PMMA breaks much less brittle compared to a high  $M_w$  PMMA. Figure 2 gives an example for a selectively EBL exposed and developed sample after manual, crystal oriented cleaving of the PMMA film being located on top of a silicon sample. After exposure with different doses and before cleaving, the samples were developed for a given time. Due to the different  $M_w$ , the development rates were also differing in the exposed sections and led to a staircase profile<sup>[3]</sup>. More interesting is the effect on the  $M_w$ .

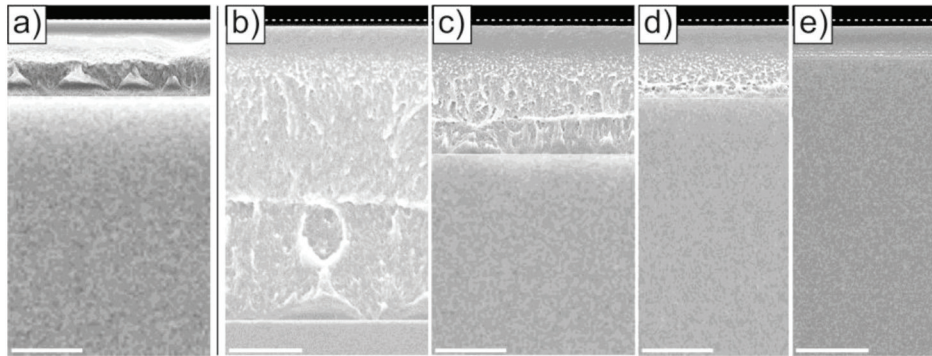


Figure 4. Comparison of a) unexposed PMMA120k with different exposed films (about 16.3 mW/cm<sup>2</sup> for 30 s) being b) 3994 nm thick, c) 1737 nm thick, d) 984 nm thick and e) 437 nm thick. The dashed line indicates the surface before exposure. (Scale bar 1  $\mu$ m)

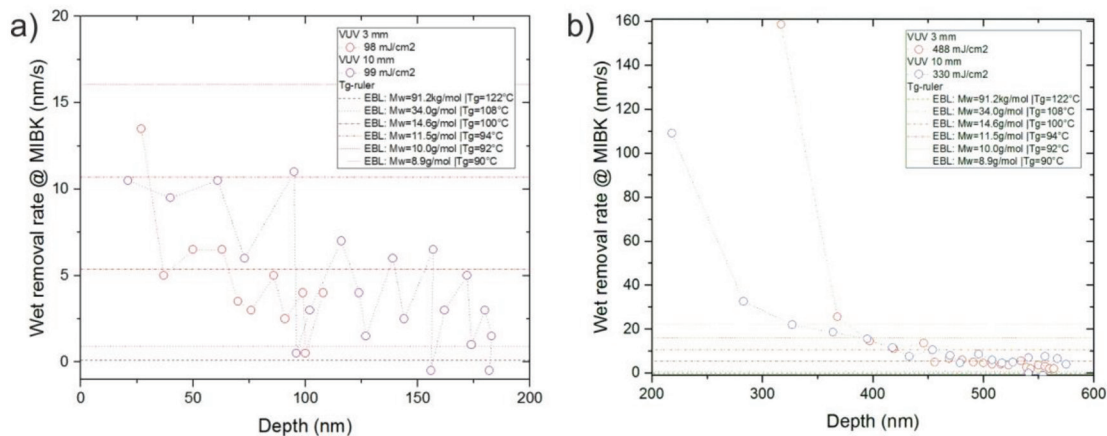


Figure 5. Plot of the solvent removal rate as depth profile measured from discrete points in time during the development process for a) low and b) much high VUV doses.

While the unexposed part ( $D_0$ ) has a rough and granular cleaving facet, this granularity decreases with increasing electron beam dose ( $D_1$ - $D_3$ ) due to a less brittle behavior of the PMMA during cleaving. The  $M_w$  regions are clearly separated in lateral direction due to the complete penetration and minimum forward scattering of the electrons in the resist due to the used 100 keV EBL system (Vistec B.V., EBP 5000 Plus).

### 2.3 Development rates

The development rate of exposed PMMA depends on the exposure dose. The higher the dose is, the lower is the  $M_w$  and the faster is the PMMA removed in a given solvent. We used the development rates for the EBL exposed PMMA120k and compared it to the development rates of the VUV exposed PMMA120k. By correlating the known  $T_g$  and the development rates for EBL exposed samples, a first rough estimation of the  $T_g$  profile of the VUV exposed samples became possible. To measure the VUV development rates, large areas were masked by a metal shadow mask and iteratively developed for 2 s in the EBL developer methyl isobutyl ketone (MIBK) and subsequently rinsed in isopropyl alcohol (IPA) to stop the development process. The depth of the developed regions was measured by stylus profilometry (Dektak 8, Veeco Inc.) after each development step. The development rates were calculated as the removed thickness per time unit.

### 2.4 Linear thermoplastic expansion

To determine the linear CTE, VUV flood exposed samples were placed on a resistive heating strip and isolated against heating of the surrounding measurement setup being placed in an optical microscope. The film thickness was measured continuously using a white light reflectometry film thickness probe (FTP, Sentech GmbH) with the microscopes 10x objective (Fig. 3a). Synchronized to the film thickness, the surface temperature of the PMMA120k sample was measured using a K-type thermocouple. The surface was continuously kept in focus for the complete measurement cycle by manual control. To minimize the effect on the sample, a yellow filter was applied to the beam path. The sample was slowly heated to a temperature above its expected  $T_g$ . For reasons of stability and accuracy, the film thickness was measured during the subsequent cooling of the samples back to room temperature. It was found that for excessively exposed samples, the film thickness continuously decreased when the temperature was kept constant for a too long time above  $T_g$ .

Due to the exponential absorption of the VUV photons, a similar exponential increase of the  $M_w$  from the surface down to the bulk can be expected. The lowest  $M_w$  chains on the surface are so small, that they become volatile and leave the sample surface during the exposure. This becomes visible by a reduced film thickness before and after exposure and the main reason for film thickness



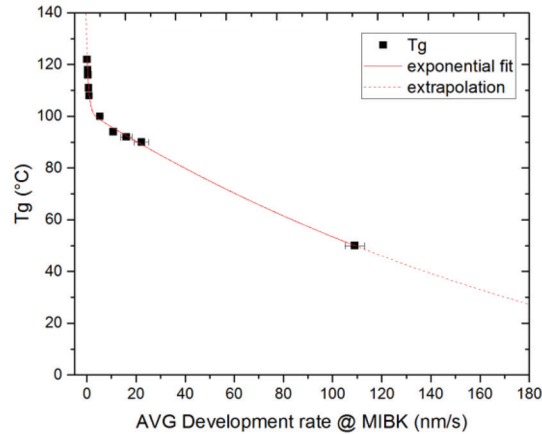


Figure 6. Consolidated plot of EBL obtained development rates (< 30 nm/s) and a VUV exposure with an averaged  $T_g$  estimation (109 nm/s) using a double exponential decay to fit and to extrapolate the data for a rough  $T_g$  estimation. The estimation assumes an almost linear relation between  $T_g$  and development rate below the critical molecular weight of PMMA which is estimated to be about  $M_w \sim 15 \text{ kg/mol}^{[2]}$  giving a removal or development rate of about 10 nm/s.

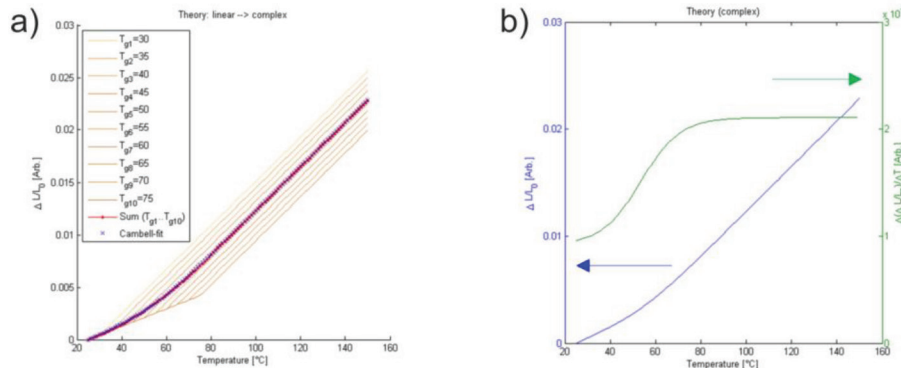


Figure 7. Comparison of a) the summed material behavior of a ten-layer stack with a  $T_g$  range from 30°C to 75°C and b) the fitted Campbell equation (Eq. (1)) for this material stack together with the derived CTE.

reduction and instabilities during the measurement process. This is also the limitation of the used measurement system: very low  $T_g$  values of the most upper material cannot be captured as this material evaporates immediately during the measurement. The remaining material has also no homogenous CTE as this CTE strongly depends on the  $T_g$  and thus the  $M_w$  depth profile. The exposed material can be imagined as a stack of films with a different CTE for each film and an infinitely small thickness per layer. In conclusion, the FTP measurements capture all CTEs of this material stack in an integrative manner. In consequence, one can extract the film thickness and the CTE change versus the temperature (Fig. 3b).

For simplicity, the refractive index was assumed to be constant over temperature which is the reason for a certain but acceptable inaccuracy of the measured values and part of ongoing process improvement.

## 2.5 Surface confined reflow and device fabrication

Optical diffuser structures and micro-prism reflectors were fabricated by direct laser writing using multi-photon lithography (MPL) and the obtained patterns were replicated from the MPL resist into the PMMA120k by nanoimprint lithography using elastomeric molds and hot embossing<sup>[4,11,13]</sup>. The negative tone MPL resist could not be treated in a similar way as describe here and thus required the pattern transfer into PMMA. This made the op-

tical structures accessible for polymer reflow. The VUV exposed samples were globally heated on hotplate using a top-heater setup to additionally enhance the viscosity gradient from top to bottom of the structure due to the temperature gradient generated with the topheater setup<sup>[11]</sup>.

## 3. Results and Discussion

### 3.1 Profile of SEM cross sections

SEM cross sections indicated only a minimal removal of about 20 nm PMMA120k within 30 s of exposure in a distance of 3 mm to the lamp housing. For the intended smoothening of micro-optics this has only a neglectable influence on the device performance. The average thickness of the visible film modification was about  $298 \pm 11 \text{ nm}$  for different film thicknesses between 437 nm and 3994 nm (Fig. 4). This confirms an expected, constant modification thickness independent of the film thickness itself due to the exponential attenuation of the VUV photons starting from the top of the film. This exponential intensity decay is also visible in Figure 4 comparing the films ranging from the thickest (Fig. 4b) down to the thinnest film (Fig. 4e). The cleaving itself generates, in dependence of the  $M_w$ , additional facet features being mostly located close to the substrate. However, comparing the less affected upper part of each thickness shows very similar features

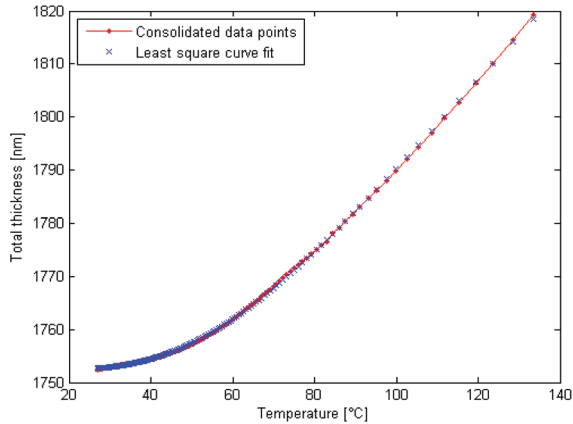


Figure 8. Thickness change of an initially 1750 nm thick PMMA120k film after heating up to 135°C and being measured during the subsequent cooldown.

among all thicknesses: a completely smooth facet on top with a continuous transition towards more granular and finally very rough facet well below the surface. This top 298 nm are, hence, most affected by the VUV photons. However, below this region there is evidence from this cross sections, that the modification is ranging more than 1  $\mu\text{m}$  deep but has probably no significant effect on the  $T_g$  in this depth compared to the top 298 nm.

### 3.2 Development rates

In dependence of the exposure dose ranging from 98  $\text{mJ}/\text{cm}^2$  up to 488  $\text{mJ}/\text{cm}^2$ , the development rates strongly increased and exceeded by far the rates found for the 100 keV electron beam exposed samples (Fig. 5). This is in agreement with literature findings that photons of about 190 nm wavelength are much more efficient in chain scission compared to 25 keV and thus even more pronounced compared to 100 keV electrons<sup>[14]</sup>. It is well known, that a higher acceleration voltage in EBL leads to a reduced sensitivity for the same resist material. While for low VUV doses of about 100  $\text{mJ}/\text{cm}^2$ , the  $T_g$  was well in the range of the EBL samples and did not exceed 90°C in the most upper PMMA region (Fig. 5a), doses above 100  $\text{mJ}/\text{cm}^2$  resulted in a much more pronounced  $T_g$  reduction (Fig. 5b). For the smaller doses an almost linear decay of the  $T_g$  is visible reaching the bulk behavior already about 200 nm from the top surface. While this is not sufficient to efficiently reduce roughness in the 100 nm range without influencing the bulk material, the higher doses create a more useful, significant contrast between the top film and the bulk. The  $T_g$  drops almost exponentially with a quite sharp transition about 300 nm to 400 nm from the surface. Using even more dose will enhance this contrast and also increase the modified film thickness but ultimately will lead to a strong ablation or etching of the film surface. This ablation limit defines the maximum dose that can be used for material modification without significant shape deterioration of an optical device.

Regarding the  $T_g$  values determined for EBL<sup>[3]</sup> (cf. Fig. 2), the generally much larger development rates suggest a much lower  $T_g$  for the VUV exposed samples compared to the EBL samples. A rough estimation based on the extrapolation of the EBL sample  $T_g$  values using the EBL development rates and a VUV exposure with known development rate (Fig. 6) places the VUV  $T_g$  in the range of 30°C to 40°C in the top surface for the high dose VUV exposure. An improved  $T_g$  measurement is expected from CTE setup.

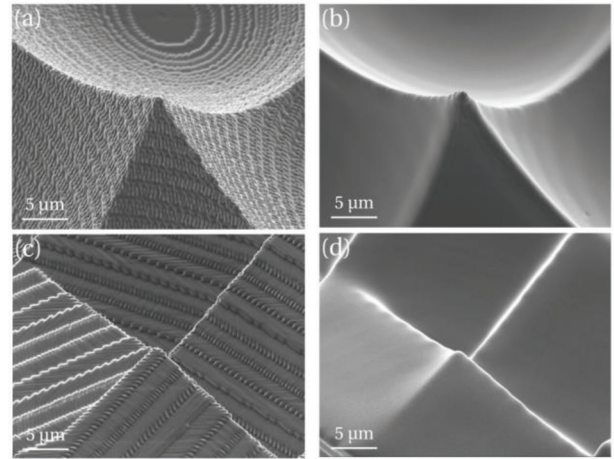


Figure 9. Two optical devices (micro-lens and micro-prism) replicated into PMMA120k from the MPL resist via intermediate molds and subsequently smoothed in a surface confined reflow process and depicted a), c) before and b), d) after reflow.

### 3.3 Glass transition temperature

For simplification, we assumed a discrete layering as depth profile instead of a continuous change of the  $T_g$  versus the depth. Figure 7a shows the representative plot of the relative thickness change over temperature for an idealized and theoretical stack of ten layers with the  $T_g$  ranging from 30°C to 75°C in these layers. Below the respective  $T_g$  the CTE is constant and above as well but with a steeper gradient. Assuming that all layers contribute equally to the film thickness increase gives the summed thickness behavior depicted also in Figure 7a. This summed behavior can be well modelled using the equation derived by Campbell et al.<sup>[15]</sup> for the temperature dependent thickness  $h(T)$  of a thin film:

$$h(T) = w \left( \frac{M - G}{2} \right) \ln \left( \cosh \left( \frac{T - T_g}{w} \right) \right) + (T - T_g) \left( \frac{M + G}{2} \right) + c \quad (1)$$

In this equation,  $w$  is the width of the glass transition region,  $M$  is the CTE of the melt (above  $T_g$ ),  $G$  is the CTE in the glassy region (below  $T_g$ ),  $T_g$  is the glass transition temperature itself and  $c$  is the film thickness at  $T_g$ . We used a full parameter, least-square fit of the measured data to this equation by Matlab® routines. Figure 7a shows, that the fit result for the summed behavior of the ten-layer stack can exactly describe the theoretical material behavior. For a full depth profile, the thickness of the individual layers would need to be fitted as well using an improved model. However, this is beyond the scope of this contribution and part of ongoing work. However, the model gives already as major output of the fit both the central  $T_g$  and the width  $w$  of the glass transition region. For the theoretical stack of the ten layers, the determined  $T_g$  region was 52.5±22.5 °C. Figure 7b gives the respective derivative and thus CTE for this fitted sum signal. This result is exactly the average of the lowest and the largest  $T_g$  in the stack as central  $T_g$  and the width being defined by both extreme values. Thus, from the Campbell fit so far the largest and the lowest  $T_g$  in the complete stack can be extrapolated.

Figure 8 shows the consolidated data points and the least square fit for a 1750 nm thick PMMA120k film after exposure. Two distinct features can be seen in this graph: First, there is a clear  $T_g$  region present due to the almost constant thickness change beyond 80°C. Second, the  $T_g$  transition region is rather larger and no linear section below a certain lower temperature limit is present.

Indeed, the *Campbell* fit gave a  $T_g$  region of  $49\pm 33^\circ\text{C}$  with  $16^\circ\text{C}$  as lowest and  $82^\circ\text{C}$  a largest  $T_g$  in this stack. As mentioned above, the model does so far not provide the thickness of the respective regions. However, it confirms that the  $T_g$  region extends to room temperature and thus the lower measurable limit of this setup. Considering the very low  $M_w$  compounds that have already been removed during the exposure, the very top layers must be just at the limit of volatility under the exposure conditions and thus must have a very low  $T_g$ . The upper limit of  $82^\circ\text{C}$  is very close to the  $T_g$  of about  $90\text{--}96^\circ\text{C}$  measured for the unexposed PMMA with this setup. This is close to the  $T_g$  of  $101^\circ\text{C}$  measured by differential scanning calorimetry for the bulk PMMA120k material that is used to prepare the spincoating solutions. The model is at the moment limited to constant refractive indices which partly explains the difference in the here measured bulk  $T_g$  as compared to  $122^\circ\text{C}$  measured elsewhere under different conditions<sup>[3]</sup>. As conclusion, so far a continuous  $T_g$  increase from the top towards the substrate is present with very low  $T_g$  values of about room temperature at the surface.

### 3.4 Device reflow

Based on the knowledge of this very low  $T_g$  top layer, a smoothening of initially very rough surfaces (Fig. 9a,c) into ultra-smooth and optical grade surfaces was achieved (root mean square roughness below 10 nm) (Fig. 9b,d). For this, an intensive exposure for 30 s in a distance of 3 mm was used to enable a significant material modification. The reflow took place at  $140^\circ\text{C}$  for 15 min. This post-processing allows a significant time saving during the MPL process. While a rather coarse surface as in Figure 9a,c can be written very fast, a smooth surface similar to Figure 9b,d requires an about ten time longer MPL writing process<sup>[11]</sup>. Replication into PMMA, post-processing by VUV exposure and global thermal heating as well as the final replication into the product material is mostly still more efficient than the extended writing time. To understand this, one has to consider that a replication process chain often needs to be established for the high volume manufacturing of micro-optical elements. Once this process chain is in place, the additional steps introduced by our post-processing do not significantly extend the process time and rather save a lot of time during the fabrication of the original patterns used for replication. However, there might be cases that could not effort such a post-processing due to the low volume of fabricated structures and rather use extended direct writing of the required structures.

## 4. Conclusion

We assessed the glass transition temperature distribution in a VUV exposed sample and found that the total modified film thickness might reach down to more than 500 nm but with the most significant region being about the top 300 nm of the exposed PMMA films. In this region, the  $T_g$  is extremely reduced almost down to room temperature and this enables a surface selective reflow that does not alter the overall micron-scale shape and rather removes selectively the superficial roughness of micro-optical devices. The achieved material modification fits very well the typical roughness of microfabrication processes. For other processes, the penetration depth can be adjusted with the dose, but this has a direct impact on the  $T_g$  contrast, or by using another exposure wavelength with a different penetration characteristic. The presented method is of largest interest for the high volume fabrication of micro-optical devices using polymer replication techniques such as hot embossing, UV-molding or injection molding.

## 5. Acknowledgements

This project was funded by the Swiss Nanoscience Institute (project A10.13 SurfFlow). The authors express their special thanks to K. Vogelsang (PSI) for support with the hot embossing. The authors also thank M. Rossi (Heptagon) for the support of this project and the useful discussion.

## 6. References

- [1] Dobisz, E.A., Brandow, S.L., Bass, R., and Mitterender, J., "Effects of molecular properties on nanolithography in polymethyl methacrylate," *J. Vac. Sci. Technol. B*, 18, 107–111 (2000).
- [2] Fuchs, K., Friedrich, C., and Weese, J., "Viscoelastic properties of narrow-distribution poly(methyl methacrylates)," *Macromolecules* 29, 5893–5901 (1996).
- [3] Schleunitz, A., Guzenko, V.A., Messerschmidt, M., Atasoy, H., Kirchner, R., and Schiff, H., "Novel 3D micro and nanofabrication method using thermally activated selective topography equilibration (TASTE) of polymers," *Nano Convergence* 1:7, 1–8 (2014).
- [4] Chidambaram, N., Kirchner, R., Fallica, R., Yu, L., Altana, M. and Schiff, H., "Selective Surface Smoothening of Polymer Microlenses by Depth Confined Softening", *Adv. Mater. Technol.* 2(5), 1700018 (2017).
- [5] Ishihara, Y., and Tanigaki, K., "A high photosensitive IL-CCD image sensor with monolithic resin lens array," *Proc. Int. Electron Devices Meeting* 29, 497–500 (1983).
- [6] Popovic, Z.D., Sprague, R.A., and Connell, G. A. N., "Technique for monolithic fabrication of microlens arrays," *Appl. Opt.* 27, 1281–1284 (1988).
- [7] Kirchner, R., Schleunitz, A., and Schiff, H., "Energy-based thermal reflow simulation for 3D polymer shape prediction using the surface evolver," *J. Micromech. Microeng.* 24(5), 055010 (7pp) (2014).
- [8] Kirchner, R., and Schiff, H., "Mobility based 3D simulation of selective, viscoelastic polymer reflow using Surface Evolver," *J. Vac. Sci. Technol.* 32(6), 06F701 (7pp.) (2014).
- [9] Schiff, H., Chidambaram, N., Altana, M., and Kirchner, R., "Selective surface smoothening of 3D micro-optical elements", *Proc. SPIE* 10144, 101440B (2017).
- [10] Kirchner, R., Chidambaram, N., Altana, M., and Schiff, H., "How post-processing by selective thermal reflow can reduce the roughness of 3D lithography in micro-optical lenses," *Proc. SPIE* 10095, 1009507 (2017).
- [11] Kirchner, R., Chidambaram, N., and Schiff, H., "Surface selective VUV and thermal post-processing of thermoplastics for ultra-smooth 3D-printed micro-optics," submitted to *Opt. Eng.* (2017).
- [12] Kahle, O., Wielsch, U., Metzner, H., Bauer, J., Uhlig, C., and Zawatzki, C., "Temperature and thermal expansion behavior of polymer films investigated by variable temperature spectroscopic ellipsometry," *Thin Solid Films* 313–314, 803–807 (1998).
- [13] Chidambaram, N., Kirchner, R., Altana, M., and Schiff, H., "High fidelity 3D thermal nanoimprint with UV curable polydimethyl siloxane stamps," *J. Vac. Sci. Technol. B* 34(6), 06K401 (2016).
- [14] Choi, L.O., Moore, J.A., Corelli, J.C., Silverman, J.P., and Bakhr, H., "Degradation of poly(methylmethacrylate) by deep ultraviolet, x-ray, electron beam, and proton beam irradiations," *J. Vac. Sci. Technol. B*, 6, 2286–2289 (1988).
- [15] Campbell, C. G. and Vogt, B. D., "Examination of the influence of cooperative segmental dynamics on the glass transition and coefficient of thermal expansion in thin films probed using poly(n-alkyl methacrylate)s," *Polymer* 48/24, 7169–7175 (2007).





N • E • W • S

## Sponsorship Opportunities

Sign up now for the best sponsorship opportunities

Photomask 2017 –

Contact: Melissa Farlow,

Tel: +1 360 685 5596; [melissaf@spie.org](mailto:melissaf@spie.org)

Advanced Lithography 2018 –

Contact: Teresa Roles-Meier,

Tel: +1 360 685 5445; [teresar@spie.org](mailto:teresar@spie.org)

## Advertise in the BACUS News!

The BACUS Newsletter is the premier publication serving the photomask industry. For information on how to advertise, contact:

Melissa Farlow,

Tel: +1 360 685 5596

[melissaf@spie.org](mailto:melissaf@spie.org)

## BACUS Corporate Members

Acuphase Inc.

American Coating Technologies LLC

AMETEK Precitech, Inc.

Berliner Glas KGaA Herbert Kubatz GmbH & Co.

FUJIFILM Electronic Materials U.S.A., Inc.

Gudeng Precision Industrial Co., Ltd.

Halocarbon Products

HamaTech APE GmbH & Co. KG

Hitachi High Technologies America, Inc.

JEOL USA Inc.

Mentor Graphics Corp.

Molecular Imprints, Inc.

Panavision Federal Systems, LLC

Profilocolore Srl

Raytheon ELCAN Optical Technologies

XYALIS

# Industry Briefs

## ■ Mycronic Receives Largest Multiple Mask Writer Order

Mycronic AB has received an order of multiple mask writers from Photronics, Inc. The order, which combines manufacturing and quality control of the most advanced small and large photomasks, comprises one mask writer Precision-800, one mask writer Precision-10, one measurement system Precision-MMS as well as a refurbished Precision-10.

This is the largest order ever for Mycronic and the total value of this combination deal is in the range of \$90 to \$100 million. All systems except the Precision-MMS are scheduled to be delivered during 2018. The Precision-MMS will be delivered during the first half of 2019. All systems will be shipped to Asia, three of them to China while the Precision-800 will be placed in South Korea.

Mycronic's most advanced mask writer, the Precision-800, enables more than 25 percent denser pattern designs than previously possible. This system will ensure efficient production of future display photo-masks for such products as 4K smartphone displays and advanced AMOLED displays.

According to Magnus Råberg, Sr VP and General Manager Pattern Generators of Mycronic AB, manufacturers are investing in a growing Chinese display industry. There are 27 display fabs in China and approximately 15 new display fabs are being constructed or planned, many of them targeting large format LCD displays for TV or AMOLED for mobile devices. Photronics previously announced it has decided to invest USD 160 million in the most advanced display photomask factory in China. At the same time, the trend towards displays with higher resolution has accelerated and display technologies have become more advanced. Photronics is the first customer to use Precision-800.

<http://www.icconnect007.com>

## ■ Samsung Strengthens Advanced Foundry Portfolio

SEOUL, South Korea--(BUSINESS WIRE)--Samsung Electronics Co., Ltd., announced it has added 11-nanometer (nm) FinFET process technology (11LPP, Low Power Plus) to its advanced foundry process portfolio. Through this, Samsung has completed a comprehensive process roadmap spanning from 14nm to 11nm, 10nm, 8nm, and 7nm in the next three years."

Through further scaling from the earlier 14LPP process, 11LPP delivers up to 15 percent higher performance and up to 10 percent chip area reduction with the same power consumption. In addition to the 10nm FinFET process for mobile processors in premium flagship smartphones, the company expects its 11nm process to bring differentiated value to mid- to high-end smartphones. Samsung also confirmed that development of 7LPP with EUV (extreme ultra violet) lithography technology is on schedule, targeting its initial production in the second half of 2018.

Since 2014, Samsung has processed close to 200,000 wafers with EUV lithography technology and, building on its experience, has recently seen visible results in process development such as achieving 80 percent yield for 256 megabit (Mb) SRAM (static random-access memory).

<http://www.businesswire.com>

## ■ ASML Cranks Up Output of 'Extreme' Chipmaking Machines

FRANKFURT, Germany — ASML, the world's leading supplier of equipment for etching circuits onto silicon chips, is starting to mass-produce eagerly awaited next-generation machinery that will enable giants like Intel and Samsung Electronics to churn out more powerful semiconductors. The new equipment sells for 100 million euros (\$119 million) or more per unit.

ASML shipped a total of 14 EUV lithography units from 2013 through 2016, mainly as trial products for chipmakers. With mass production getting underway, the Dutch company expects to ship 12 units in 2017 and 24 units in 2018.

Many customers have started buying the equipment for commercial chip production, Executive Vice President Frits van Hout told The Nikkei. Van Hout said he expects the machines to become part of the industry mainstream quickly.

EUV technology has faced technological hurdles, including in the speed of wafer processing. But weaknesses in productivity and elsewhere have been overcome, van Hout said. Units can now process 2,000 wafers per day, he said. The company's moves to strengthen its EUV lithography technology include acquiring Taiwan-based Hermes Microvision last year.

Putting EUV equipment into mass production will solidify ASML's lead in chip lithography, which amounts to a roughly 80% share of the global market. Japan's Nikon, which once held the crown, beat an early retreat from EUV machinery development and focused instead on its own miniaturization technology. But massive cost burdens from that effort led to continued losses. Nikon has announced moves including staff cutbacks and scaled-back development of next-generation equipment and is shifting to build-to-order manufacturing.

<http://asia.nikkei.com>



# Join the premier professional organization for mask makers and mask users!

## About the BACUS Group

Founded in 1980 by a group of chrome blank users wanting a single voice to interact with suppliers, BACUS has grown to become the largest and most widely known forum for the exchange of technical information of interest to photomask and reticle makers. BACUS joined SPIE in January of 1991 to expand the exchange of information with mask makers around the world.

The group sponsors an informative monthly meeting and newsletter, BACUS News. The BACUS annual Photomask Technology Symposium covers photomask technology, photomask processes, lithography, materials and resists, phase shift masks, inspection and repair, metrology, and quality and manufacturing management.

### Individual Membership Benefits include:

- Subscription to BACUS News (monthly)
- Eligibility to hold office on BACUS Steering Committee

[www.spie.org/bacushome](http://www.spie.org/bacushome)

### Corporate Membership Benefits include:

- 3-10 Voting Members in the SPIE General Membership, depending on tier level
- Subscription to BACUS News (monthly)
- One online SPIE Journal Subscription
- Listed as a Corporate Member in the BACUS Monthly Newsletter

[www.spie.org/bacushome](http://www.spie.org/bacushome)

C  
a  
l  
e  
n  
d  
a  
r

### 2018

- 
**SPIE Advanced Lithography**  
 25 February-1 March 2018  
 San Jose Marriott and San Jose Convention Center  
 San Jose, California, USA  
[www.spie.org/al](http://www.spie.org/al)
- 
**Photomask Japan 2018**  
 18-20 April 2018  
 Pacific Yokohama  
 Yokohama, Japan
- 
**The 34 European Mask and Lithography Conference, EMLC 2018**  
 19-20 June 2018  
 MINATEC Conference Centre  
 Grenoble, France
- 
**SPIE Photomask Technology + EUV Lithography**  
 17-21 September 2018  
 Monterey Convention Center  
 Monterey, California

SPIE is the international society for optics and photonics, an educational not-for-profit organization founded in 1955 to advance light-based science and technology. The Society serves nearly 264,000 constituents from approximately 166 countries, offering conferences and their published proceedings, continuing education, books, journals, and the SPIE Digital Library in support of interdisciplinary information exchange, professional networking, and patent precedent. SPIE provided \$4 million in support of education and outreach programs in 2016. [www.spie.org](http://www.spie.org)

### SPIE.

*International Headquarters*  
 P.O. Box 10, Bellingham, WA 98227-0010 USA  
 Tel: +1 360 676 3290  
 Fax: +1 360 647 1445  
 help@spie.org • [www.SPIE.org](http://www.SPIE.org)

*Shipping Address*  
 1000 20th St., Bellingham, WA 98225-6705 USA

### Managed by SPIE Europe

2 Alexandra Gate, Ffordd Pengam, Cardiff, CF24 2SA, UK  
 Tel: +44 29 2089 4747  
 Fax: +44 29 2089 4750  
 spieeurope@spieeurope.org • [www.spieeurope.org](http://www.spieeurope.org)

You are invited to submit events of interest for this calendar. Please send to [lindad@spie.org](mailto:lindad@spie.org); alternatively, email or fax to SPIE.